

Mechanism and kinetics of phase formation of cobalt oxyhydrates $(\text{Na,K})_x(\text{H}_2\text{O})_y\text{CoO}_{2-\delta}$ synthesized using aqueous permanganate solution route

Chia-Yi Liu,^a Wen-Chin Hung,^a Chia-Yuan Liao,^a Jung-Sheng Wang,^a and Hwo-Shuenn Sheu^b

^aDepartment of Physics, National Changhua University of Education, Changhua 500, Taiwan, R. O. C.

^bNational Synchrotron Radiation Research Center, Hsinchu 30076, Taiwan, R. O. C.

Abstract: We have synthesized the potassium sodium cobalt oxyhydrates $(\text{Na,K})_x(\text{H}_2\text{O})_y\text{CoO}_{2-\delta}$ using the aqueous KMnO_4 solution. According to the chemical analyses, it is found that a partial or even almost complete replacement of K^+ for Na^+ in the alkaline layers. Direct formation of the $c \approx 13.9\text{\AA}$ phase is apparently associated with the larger size of K^+ ($\sim 1.4\text{\AA}$) as compared to Na^+ ($\sim 1.0\text{\AA}$). It was thought that the $\text{Br}_2/\text{CH}_3\text{CN}$ route involves an oxidative de-intercalation process. However, we have found that de-intercalation of Na^+ can be simply achieved by immersing $\gamma\text{-Na}_{0.7}\text{CoO}_2$ in the tap water, which indicates that de-intercalation of Na^+ is not necessarily brought about by oxidation, instead it should be associated with the escape tendency of the Na^+ of the $2b$ site due to its stronger Na-Co Coulomb repulsion. Formation of the $(\text{Na,K})_x(\text{H}_2\text{O})_y\text{CoO}_{2-\delta}$ not only involves the de-intercalation, oxidation, and hydration process, but also an ion exchange reaction. The hydration reaction is a slow process based on a systematic study on the phase formation of $(\text{Na,K})_x(\text{H}_2\text{O})_y\text{CoO}_2$, particularly when using aqueous KMnO_4 solution with low molar ratio of KMnO_4/Na . According to the Co K-edge XANES spectra, the oxidation number of the Co for $\text{Na}_{0.33}\text{K}_{0.02}(\text{H}_2\text{O})_{1.33}\text{CoO}_{1.95}$ ($c \approx 19.6\text{\AA}$) is higher than that of $\text{Na}_{0.07}\text{K}_{0.21}(\text{H}_2\text{O})_{0.73}\text{CoO}_{1.81}$ ($c \approx 13.9\text{\AA}$) with a chemical shift of 4.1 eV, which is consistent with the iodometric titration analyses with $\text{Co}^{3.56+}$ for the former as compared to $\text{Co}^{3.34+}$ for the latter. The oxygen deficiency $\delta = 0.19$ for $\text{Na}_{0.07}\text{K}_{0.21}(\text{H}_2\text{O})_{0.73}\text{CoO}_{1.81}$ might be responsible for being unable to form the $c \approx 19.6$ phase due to being unable to stabilize the hydrated structure of bilayers of water molecule in the lattice.

Introduction

The discovery of superconductivity of $\text{Na}_{0.35}(\text{H}_2\text{O})_{1.3}\text{CoO}_{2-\delta}$ with $T_c \approx 4\text{--}5\text{ K}$ by Takada et al.¹ is a surprise after several years of studies on the potential thermoelectric materials $\gamma\text{-Na}_x\text{CoO}_2$.² The parent material of $\gamma\text{-Na}_{0.7}\text{CoO}_2$ crystallizes in a hexagonal lattice with the space group of $\text{P6}_3/\text{mmc}$ (#194) and belongs to a category of $\gamma\text{-Na}_x\text{Co}_y\text{O}_2$ phase with $0.55 \leq x/y \leq 0.74$ (also classified as P2 phase).³ The sodium is considered as a charge reservoir and located between CoO_2 layers with prismatic surroundings. There are two different sites for the sodium in the crystallographic positions, which are usually not fully occupied by the sodium and hence have vacancies on them, however also make this class of compounds more complicated in structure and rich in properties. The Co ions form a layered triangular sublattice, on which geometric frustration of antiferromagnetic arrangement could occur. In the presence of strong correlation of 3d electrons of Co ions, the magnetic geometric frustration is of particular interest and could be associated with the unusual electronic, thermoelectric, and magnetic properties.^{2,4,5}

The superconducting phase of fully hydrated $\text{Na}_{0.35}(\text{H}_2\text{O})_{1.3}\text{CoO}_{2-\delta}$ was obtained by immersing $\gamma\text{-Na}_{0.7}\text{CoO}_2$ powders in $\text{Br}_2/\text{CH}_3\text{CN}$ solution followed by filtering and rinsing.¹ Upon intercalation, the c -axis of the parent compound $\gamma\text{-Na}_{0.7}\text{CoO}_2$ expands from 10.9\AA to 19.6\AA to form the fully hydrated sodium cobalt oxyhydrates $\text{Na}_{0.35}(\text{H}_2\text{O})_{1.3}\text{CoO}_{2-\delta}$ with bilayers of water molecules intercalated into host lattice. Since the fully hydrated phase preserves the structural integrity of the host lattice, the reaction can be viewed as a topotactic transformation process. Formation of superconducting $\text{Na}_{0.35}(\text{H}_2\text{O})_{1.3}\text{CoO}_{2-\delta}$ is generally considered as an oxidative deintercalation by removing Na^+ partially from the host lattice, followed by a hydration reaction. It is well known that KMnO_4 is a strong oxidizing agent

with a unique affinity for oxidizing organic compounds, which is particularly useful for in-situ remediation of organic compounds in ground water and subsurface soils when coupled with delivery techniques. We have recently reported that superconducting cobalt oxyhydrates with $c \approx 19.6\text{\AA}$ can be obtained by immersing $\gamma\text{-Na}_{0.7}\text{CoO}_2$ either in the aqueous KMnO_4 or NaMnO_4 solution without resort to the volatile and flammable $\text{Br}_2/\text{CH}_3\text{CN}$ solution.^{6,7} As shown in Fig. 1, a new phase of cobalt oxyhydrates $(\text{Na,K})_x(\text{H}_2\text{O})_y\text{CoO}_{2-\delta}$ with $c \approx 13.9\text{\AA}$ can be directly obtained when the molar ratio of KMnO_4 relative to the Na content in the parent compound is equal to or greater than 4.286 ($\text{KMnO}_4/\text{Na} \geq 4.286$).⁸ It should be noted that the $c \approx 13.9\text{\AA}$ phase with the mono-layers of water molecules residing within the alkaline metal layers cannot be directly obtained by using aqueous NaMnO_4 solution even at the molar ratio of $\text{NaMnO}_4/\text{Na} = 40$.²⁴ It is now known that the superconducting cobalt oxyhydrates is not stable with respect to the ambient conditions, applied pressure and evacuation.^{9,10} When subjecting to heating, pressure, or evacuation, the $c \approx 19.6\text{\AA}$ phase of the fully hydrated cobalt oxyhydrates tends to lose water and transforms into the $c \approx 13.9\text{\AA}$ phase however preserving the structural integrity with little change of the a -axis. With the direct synthesis of the $c \approx 13.9\text{\AA}$ phase, it is therefore interesting to study the mechanism and kinetics of the phase formation of mixed alkaline metal cobalt oxyhydrates. In the course of careful studies, we have found that the de-intercalation of Na^+ first occurs and proceeds relatively fast and leads to the non-hydrate phase of $c \approx 11.2\text{\AA}$. It was commonly thought that the de-intercalation of Na^+ from the parent compound would need the actions by the oxidants such as Br_2 or KMnO_4 . Surprisingly, it can be achieved by simply immersing $\gamma\text{-Na}_{0.7}\text{CoO}_2$ in the tap water. In contrast to the fast de-intercalation, the subsequent hydration is a slow process and results in the $c \approx 19.6\text{\AA}$ phase, particularly when using a low molar ratio of KMnO_4/Na . At sufficiently high molar ratio of KMnO_4/Na , partial

or almost complete substitution of K^+ for Na^+ via an ion exchange process leads to the $c \approx 13.9$ Å phase due to the size effects. Therefore, formation of the mixed alkaline metal cobalt oxyhydrates not only involves the oxidative deintercalation and hydration reaction but also the ion exchange reaction in one pot using the aqueous $KMnO_4$ solution route.

Experimental Section

Preparation of materials. Polycrystalline parent compounds of sodium cobalt oxides $\gamma\text{-Na}_{0.7}\text{CoO}_2$ were prepared using a rapid heat-up procedure in order to avoid the loss of Na in the heating process.⁸ High purity powders of Na_2CO_3 (Aldrich) and CoO (SDIC) were thoroughly mixed and ground using a Retch MM2000 laboratory mixer mill and calcined in a preheated box furnace at 800°C for 12 h. The resulting powders (0.5 -1 g) were immersed and stirred in 50 - 680 ml of aqueous $KMnO_4$ solution with different molar ratios of $KMnO_4/Na$ labeled as 0.05X – 40X at room temperature for 5 days. It should be mentioned that high molar ratio of $KMnO_4/Na$ would need more water to dissolve $KMnO_4$ due to the limited solubility of $KMnO_4$ in water. For the 40X sample, it would need 680 ml water to completely dissolve $KMnO_4$. The products were filtered and washed by de-ionized water several times with the total volume of 150-200 cc. Note that the contents of potassium and sodium of the products depend slightly on the volume of water in the washing process because they would lose a little in the water as confirmed by ICP analyses. The powders were then stored in a wet chamber with relative humidity of 98% to avoid loss of the water content.

Characterization of materials. Powder X-ray diffraction (XRD) patterns were obtained using a Shimadzu XRD-6000 diffractometer equipped with Fe K α radiation. The data were collected over the range $5^\circ \leq 2\theta \leq 90^\circ$ with 0.02° 2θ steps. The unit cell parameters were computed using a Rietveld structure refinement program, Rietica. Elemental compositions of the resulting products were determined by using a Perkin Elmer Optima 3000 DC inductively coupled plasma - atomic emission spectrometer (ICP-AES). Thermogravimetric analysis (TGA) was carried out to determine the water content of the resulting products by using a Perkin Elmer Pyris 1 thermogravimetric analyzer at a heating rate of $0.1^\circ\text{C}/\text{min}$ in flowing oxygen. X-ray absorption spectra were recorded at wiggler beamline BL17C at National Synchrotron Radiation Research Center Taiwan using transmission mode (two ionization chambers) on the powder samples. The X-ray absorption measurements were carried out at Mn and Co K-edge using the Si (111) double-crystal monochromator. The energy calibration was made according to the K-edge of the Mn and Co foils. The threshold energy (E_0) was obtained from their first derivatives of the near edge spectra. The Extended X-ray Absorption Fine Structure (EXAFS) data were analyzed following a standard procedures by FEFF program.¹¹ $\chi(E)$ of the EXAFS function was obtained by subtracting the post-edge background from the overall absorption and then normalized with respect to the edge jump step. The normalized $\chi(E)$ was transformed from energy space (eV) to k space (cm^{-1}), where k is the photoelectron wave vector. The $\chi(k)$ data could be used to

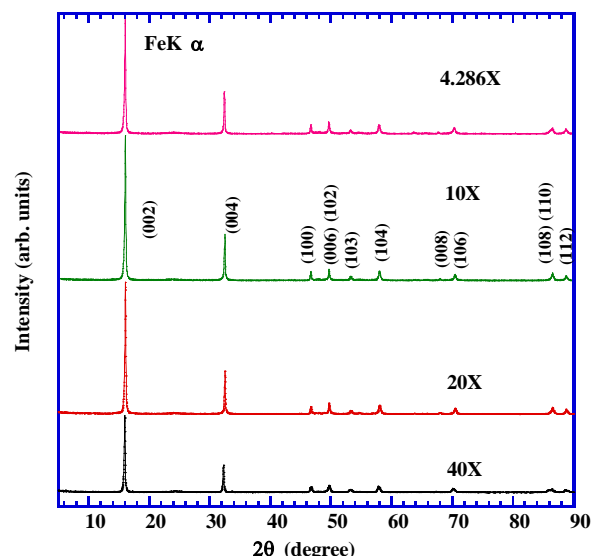


Figure 1. Powder x-ray diffraction patterns of $(Na,K)_x(H_2O)_yCoO_{2-\delta}$ obtained by immersing $\gamma\text{-Na}_{0.7}\text{CoO}_2$ in high molar ratio of aqueous $KMnO_4$ solution with respect to the Na content in the parent compound ($4.286 \leq KMnO_4/Na \leq 2.29$).

describe the oscillation of the backscattering wave through the local environment. For our samples in this study, the k^3 -weighted EXAFS spectra, $k^3 \cdot \chi(k)$, of the selected absorber Mn and Co, were calculated to compensate the damping of EXAFS oscillations in the high-k region. Subsequently, k^3 -weighted $\chi(k)$ data were Fourier transformed (FT) to r -space, in which bond distance and coordination number could be obtained.

Results and discussion

It has been previously shown that the size of molar ratio of $KMnO_4/Na$ is associated with the phase formation of $(Na,K)_x(H_2O)_yCoO_{2-\delta}$.^{6,8} According to the XRD patterns, it can be classified as four categories by the molar ratio of $KMnO_4/Na$ used to treat the parent material, i.e., $KMnO_4/Na \leq 0.1$, $0.3 \leq KMnO_4/Na \leq 0.4$, $0.5 \leq KMnO_4/Na \leq 2.29$, and $4.286 \leq KMnO_4/Na \leq 40$. After immersing $\gamma\text{-Na}_{0.7}\text{CoO}_2$ in the $KMnO_4$ solution for 5 days, the XRD patterns of the 0.05X and 0.1X show a mixture of the $c \approx 19.6$ Å phase and the $c \approx 11.2$ Å phase; the XRD patterns of the 0.3X and 0.4X samples show a pure $c \approx 19.6$ Å phase; the XRD patterns of the 0.5X, 1.529X, and 2.29X samples show a mixture of the $c \approx 19.6$ Å and the $c \approx 13.9$ Å phase; and the XRD patterns of the 4.286X, 10X, 20X, and 40X samples show a pure $c \approx 13.9$ Å phase. Moreover, we find that when storing the as-prepared 0.05X and 0.1X samples in a wet chamber with a relative humidity of 98% for a long period of time, the $c \approx 19.6$ Å phase grows at the expense of the $c \approx 11.2$ Å phase. This result indicates that intercalation of the water molecules could undergo a gas-solid interaction in addition to that through a liquid-solid reaction.

De-intercalation. On formation of superconductive $Na_{0.35}(H_2O)_{1.3}CoO_{2-\delta}$, it was generally thought that the bromine acts as the oxidizing agent by oxidizing the Co ions and leads to the de-intercalation of Na^+ from the host lattice of $\gamma\text{-Na}_{0.7}\text{CoO}_2$, which has been suggested as a process of oxidative de-

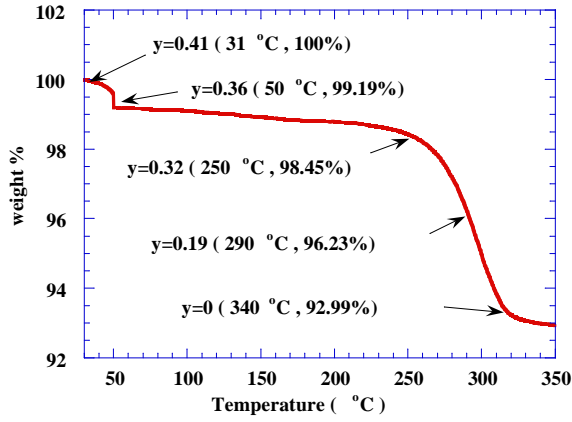


Figure 2. TGA curve of the de-intercalated samples of $\text{Na}_x(\text{H}_2\text{O})_{0.41}\text{CoO}_{2-\delta}$ obtained by immersing $\gamma\text{-Na}_{0.7}\text{CoO}_2$ in the tap water.

intercalation. In fact, de-intercalation of Na^+ can be achieved by simply immersing $\gamma\text{-Na}_{0.7}\text{CoO}_2$ in the tap water. The ICP-AES and TGA (Fig. 2) results show that the resulting product of immersing $\gamma\text{-Na}_{0.7}\text{CoO}_2$ in the tap water has the composition of $\text{Na}_{0.29}(\text{H}_2\text{O})_{0.41}\text{CoO}_{1.78}$. The spontaneous de-intercalation of Na^+ from the host lattice might be due to the stronger Na-Co Coulomb repulsion for Na^+ in the $2b$ site as compared that of $2d$ site, which makes $\gamma\text{-Na}_{0.7}\text{CoO}_2$ have the escape tendency of Na^+ when immersed in a solution. The iodometric titration shows the transition metal ions having the oxidation number of $\text{Co}^{3.27+}$. After de-intercalating some of the Na^+ from the host lattice, the coulomb attraction between the positive charges of Na^+ and the negative charges of O^{2-} becomes smaller and consequently results in a slight expansion along the c -axis. This phenomenon is observed in Fig. 3. The (002) reflection of the tape water-treated sample is found to shift to a lower angle at $2\theta = 20.02^\circ$ ($d = 5.569 \text{ \AA}$) as compared to $2\theta = 20.44^\circ$ ($d = 5.456 \text{ \AA}$) for $\gamma\text{-Na}_{0.7}\text{CoO}_2$. In case of using the aqueous KMnO_4 solution, de-intercalation of alkaline metal is readily seen in Table I, which summarizes the chemical compositions obtained by the ICP-AES analyses and the lattice parameters of KMnO_4 -prepared $(\text{Na},\text{K})_x(\text{H}_2\text{O})_y\text{CoO}_{2-\delta}$. The sum of the sodium and potassium falls in the range of 0.28 and 0.38 in terms of the molar ratio with respect to cobalt. Moreover, it can be seen that more alkaline metal (the sum of K and Na) is de-intercalated from the host lattice with a higher molar ratio of KMnO_4/Na with respect to $\gamma\text{-Na}_{0.7}\text{CoO}_2$.

Ion exchange. Ion exchange has been defined as a process in which ions are released from an insoluble permanent material in exchange for other ions in a surrounding solution. Ion exchange involves a reversible reaction with the structural integrity of the host lattice essentially preserved throughout the process. Based on the structural and chemical analyses, the structural integrity is preserved with slight variation of the lattice constants and the Na^+ is partially replaced by K^+ , indicating the occurrence of the ion exchange between Na^+ and K^+ . As shown in Table I, it shows that the sodium content in $(\text{Na},\text{K})_x(\text{H}_2\text{O})_y\text{CoO}_{2-\delta}$ decreases significantly at the molar ratio of KMnO_4/Na equal to or greater than 4.286, whereas the potassium content increases with increasing molar ratio of KMnO_4/Na . In case of the 40X sample, the K^+ almost replaces the Na^+ completely. Therefore, the more K^+ is in the aqueous solution with respect to the Na^+ in the insoluble $\gamma\text{-Na}_{0.7}\text{CoO}_2$ (a higher molar ratio of KMnO_4/Na), the more ion exchange of K^+ for Na^+ would occur.

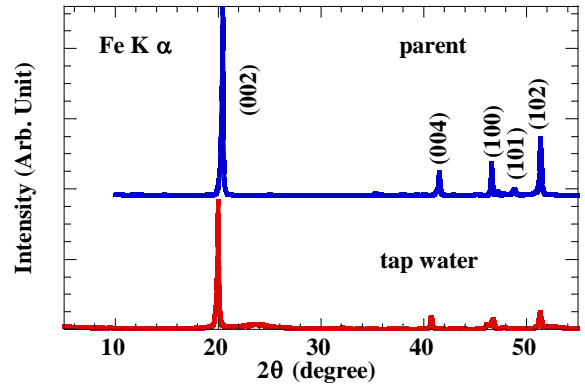


Figure 3. Powder x-ray diffraction patterns of the de-intercalated samples of $\text{Na}_{0.29}(\text{H}_2\text{O})_{0.41}\text{CoO}_{1.78}$ obtained by immersing $\gamma\text{-Na}_{0.7}\text{CoO}_2$ in tap water. The XRD pattern of parent $\gamma\text{-Na}_{0.7}\text{CoO}_2$ is also included for comparison..

Hydration. As seen in Table I, the high X samples ($\geq 4.286\text{X}$) obviously show a shorter c -axis of $\sim 13.9 \text{ \AA}$ as compared to $\sim 19.6 \text{ \AA}$ for the low X samples. In conjunction with the ICP-AES results, apparently the content of K^+ in the sample is associated with the size of the c -axis, which is reminiscent of the case in $\text{A}_x(\text{H}_2\text{O})_y\text{MS}_2$ ($\text{A} = \text{group 1A or 2A metal}$, $\text{M} = \text{Ti, Nb, or Ta}$). On contact with water vapor or with liquid water, A_xMS_2 undergoes a topotactic process and form hydrated compounds $\text{A}_x(\text{H}_2\text{O})_y\text{MS}_2$ with water molecules intercalated into the host lattice A_xMS_2 , which results in the c -axis expansion. The size of c -axis expansion is apparently associated with the size of the alkaline metal. It has been found that the alkaline metal with the ionic radius $> 1 \text{ \AA}$ would lead to bilayers of water intercalated between the MS_2 layers and hence a larger c -axis, whereas the alkaline metal with the ionic radius $< 1 \text{ \AA}$ would lead to monolayer of water inserted within the alkaline metal layers and hence a smaller c -axis.¹² The c -axis of $\text{A}_{0.3}(\text{H}_2\text{O})_y\text{TaS}_2$ is 23.63 \AA and 18.18 \AA for $\text{A} = \text{Na}^+$ (ionic radius: $\sim 1 \text{ \AA}$) and K^+ (ionic radius: $\sim 1.4 \text{ \AA}$), respectively. The interlayer height between MS_2 layers is ca. 5.77 \AA and 3.04 \AA for $\text{A} = \text{Na}^+$ and K^+ , respectively. They correspond well to once and twice the van der Waals diameter of a water molecule of $\sim 2.8 \text{ \AA}$. Similar relationships between the size of the alkaline metal and the c -axis could be found in our KMnO_4 -prepared cobalt oxyhydrates. Based on the XRD and ICP-AES results, the $c \approx 13.9 \text{ \AA}$ phase having more K^+ content has an interlayer expansion

Table I. Chemical analyses^a of ICP-AES results and lattice constants^b of $(\text{Na},\text{K})_x(\text{H}_2\text{O})_y\text{CoO}_{2-\delta}$ synthesized using aqueous KMnO_4 solution.

Molar ratio of KMnO_4/Na	K	Na	$x = \text{Na}+\text{K}$	Mn	Co	a (\AA)	c (\AA)
0.05X	0.00	0.38	0.38	0.04	1	2.8268(5)	19.626(2)
0.1X	0.01	0.34	0.35	0.07	1	2.8261(3)	19.573(1)
0.3X	0.02	0.33	0.35	0.08	1	2.8249(1)	19.669(1)
1.529X	0.05	0.31	0.36	0.07	1	2.8115(15)	19.750(5)
2.29X	0.08	0.28	0.36	0.07	1	2.8250(3)	19.735(2)
4.286X	0.18	0.15	0.33	0.07	1	2.8286(1)	13.917(1)
10X	0.21	0.07	0.28	0.08	1	2.8261(2)	13.864(1)
40X	0.25	0.03	0.28	0.08	1	2.8251(2)	13.960(1)

^aThe error in weight % of each element in ICP-AES analysis is $\pm 3 \%$, which corresponds to an estimated error of ± 0.02 per formula unit for each element.

^bThe lattice constants are obtained using Rietica, a Rietveld structure refinement program, based on a hexagonal structure ($\text{P6}_3/\text{mmc}$).

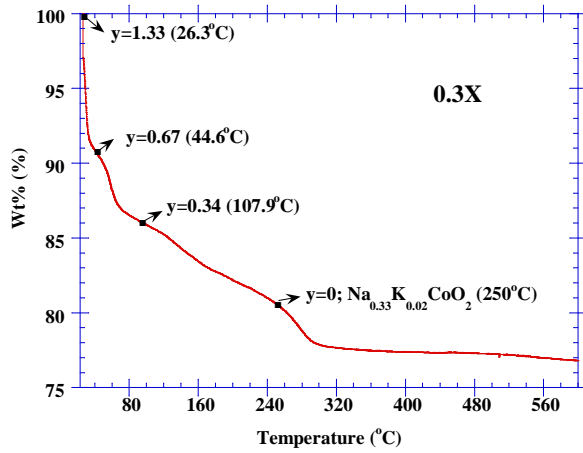


Figure 4. TGA for the 0.3X sample obtained by immersing $\text{Na}_{0.7}\text{CoO}_2$ in the aqueous KMnO_4 solution with the molar ratio of $\text{KMnO}_4/\text{Na} = 0.3$.

of ca. 1.5 Å, whereas the $c \approx 19.6$ Å phase having less K^+ content has an interlayer expansion of ca. 4.35 Å. Further evidence can be seen in the TGA results, shown in Figs. 4 and 5. The $c \approx 13.9$ Å phase has the hydration water content of $y \approx 0.73$, while the $c \approx 19.6$ Å phase has $y \approx 1.33$. Note that the water content was found to be $y \approx 0.5 - 0.7$ for $A = \text{K}$ and $y \approx 1.6 - 1.8$ for $A = \text{Na}$ in $A_x(\text{H}_2\text{O})_y\text{MS}_2$. Therefore, direct formation of $c \approx 13.9$ Å phase of cobalt oxyhydrate (Fig. 1) could be attributed to the significant increase of K^+ in the $\geq 4.286X$ samples. In addition, the KMnO_4 -prepared $c \approx 13.9$ Å phase of the high X samples cannot be transformed to the $c \approx 19.6$ Å phase by exposing the sample to a humid environment even for a long period of time. Note that the transformation between the $c \approx 13.9$ Å phase and the $c \approx 19.6$ Å phase is reversible for the low X and Br_2 -treated samples. It should be also mentioned that using aqueous NaMnO_4 solution to treat $\gamma\text{-Na}_{0.7}\text{CoO}_2$ only leads to the $c \approx 19.6$ Å phase even with the molar ratio of NaMnO_4/Na as high as 40.

Oxidation. One would expect an increase of the oxidation number of Co due to the de-intercalation of Na^+ from the host lattice. The oxidation number of cobalt has recently been determined by wet chemical analyses. The oxidation number of cobalt is +3.26 and +3.48 for $\gamma\text{-Na}_{0.77}\text{CoO}_{2.02}$ and Br_2 -treated $\text{Na}_{0.36}(\text{H}_2\text{O})_{1.33}\text{CoO}_{1.92}$, respectively.¹³ For our results determined by the iodometric titration, the oxidation number of cobalt is +3.30 and +3.56 for $\gamma\text{-Na}_{0.7}\text{CoO}_2$ and KMnO_4 -treated $\text{Na}_{0.33}\text{K}_{0.02}(\text{H}_2\text{O})_{1.33}\text{CoO}_{1.95}$, respectively. These results confirm the oxidizing role of Br_2 and KMnO_4 in increasing the oxidation number of Co. Note that the oxidation process using the Br_2 or KMnO_4 route is accompanied by the phase formation of the $c \approx 19.6$ Å phase. On the other hand, the oxidation number of cobalt is +3.27 for the tap water-treated $\text{Na}_{0.29}(\text{H}_2\text{O})_{0.41}\text{CoO}_{1.83}$ and the $c \approx 11.1$ Å is only slightly larger than the parent compound. According to the above results, the de-intercalation of Na^+ would not necessarily bring about the oxidation of Co ions or the phase formation of the $c \approx 19.6$ Å phase. Besides, one can always find the oxygen deficiency accompanying the de-intercalation of Na^+ , which is reminiscent of the case in $\text{Li}_{1-x}\text{CoO}_{2-\delta}$.¹⁴ For $\text{Li}_{1-x}\text{CoO}_{2-\delta}$, the oxygen deficiency δ increases with decreasing Li content; the oxidation number of Co increases with decreasing Li content down to $x = 0.5$ and remains almost constant. The oxygen deficiency in the sample could be considered as holes introduced into the $\text{O}^{2-}2p$ band.¹⁵ The above results for $\text{Li}_{1-x}\text{CoO}_{2-\delta}$ could be explained as follows according to ref. 14. Due to the overlap of the $\text{Co}^{3+/4+}t_{2g}$ band with the top of the $\text{O}^{2-}2p$ band, the oxidation

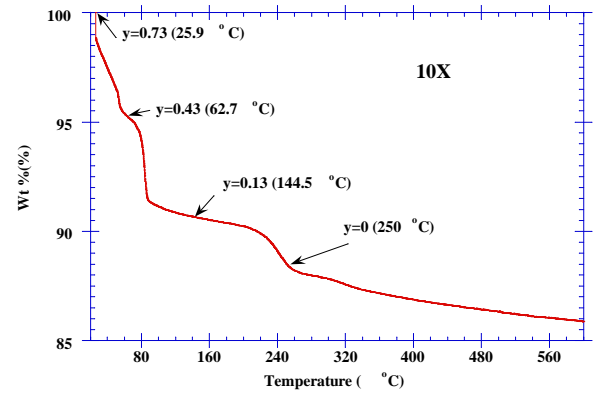


Figure 5. TGA for the 10X sample $\text{Na}_{0.07}\text{K}_{0.21}(\text{H}_2\text{O})_y\text{CoO}_{2-\delta}$ obtained by immersing $\text{Na}_{0.7}\text{CoO}_2$ in aqueous KMnO_4 solution with the molar ratio of $\text{KMnO}_4/\text{Na} = 10$. The water content is determined by assuming the complete dehydration occurring at 250°C.

is mainly occurring in the $\text{Co}^{3+/4+}t_{2g}$ band due to de-intercalation of Li^+ for $x < 0.5$, whereas further de-intercalation of Li^+ would lead to oxidation in the $\text{O}^{2-}2p$ band for $x > 0.5$ and consequently oxidizing the oxide ions to oxygen and release the oxygen from the lattice. This scenario could well be happening in the system of sodium cobalt oxide system. Oxygen vacancy is constantly observed in $\text{Na}_x\text{CoO}_{2-\delta}$ having low x values.¹⁶ The trigonal crystal field splits the threefold $\text{Co}^{3+/4+}t_{2g}$ band into a_{1g} band and twofold e_g band.¹⁷ De-intercalation of each Na^+ from the host lattice can be considered as removing an electron from the highest occupied molecular orbital (HOMO),¹⁸ which is associated with the relative energy level of $\text{Co}^{3+/4+}a_{1g}$ band with respect to the $\text{O}^{2-}2p$ band. Removing electrons from the $\text{Co}^{3+/4+}a_{1g}$ band increases the oxidation number of $\text{Co}^{3+/4+}$, whereas removing electrons from the $\text{O}^{2-}2p$ band leads to oxidation of the oxide ions and consequently the loss of oxygen from the lattice at further de-intercalation of Na^+ . In case of $\text{Na}_{0.29}(\text{H}_2\text{O})_{0.41}\text{CoO}_{1.78}$ obtained from the tap-water treatment, the electrons are presumably removed from the $\text{O}^{2-}2p$ band (see Fig. 6b) because the oxidation number of Co is +3.26 and the oxygen deficiency $\delta = 0.22$. Nevertheless, In case of $\text{Na}_{0.33}\text{K}_{0.02}(\text{H}_2\text{O})_{1.33}\text{CoO}_{1.95}$ obtained from the aqueous KMnO_4 treatment, the electrons are mainly removed from the $\text{Co}^{3+/4+}a_{1g}$ band and slightly from the $\text{O}^{2-}2p$ band (see Fig. 6a), which leads to an oxidation number of Co being +3.56 and the oxygen deficiency $\delta = 0.05$. The shifting of the $\text{Co}^{3+/4+}a_{1g}$ band relative to the $\text{O}^{2-}2p$ band could be due to the slight structural change as

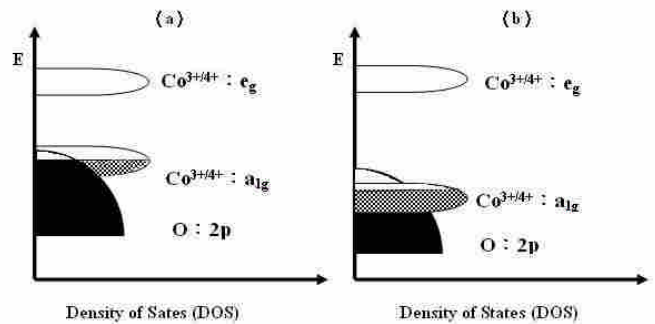


Figure 6. Possible schematic density of states diagram for $\gamma\text{-Na}_{0.7}\text{CoO}_2$ immersed in (a) aqueous KMnO_4 solution, and (b) tap water. The e_g band is not shown.

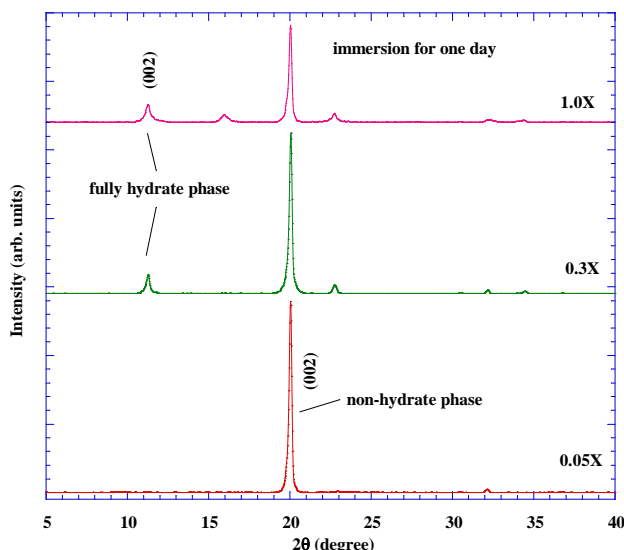


Figure 7. Powder x-ray diffraction patterns of the 0.05X, 0.3X and 1X samples which are obtained by immersing γ - $\text{Na}_{0.7}\text{CoO}_2$ in aqueous KMnO_4 solution for 1 day. The fully hydrate phase ($c \approx 19.6$ Å) is observed both in the 0.3X and 1.0X sample, indicated by the reflection peak at $2\theta \approx 11.3^\circ$, but not for the 0.05X sample. It suggests that formation of the fully hydrate phase is a very slow process when using the low concentration of aqueous KMnO_4 solution.

γ - $\text{Na}_{0.7}\text{CoO}_2$ is immersed in the tap water. As shown in Fig. 3, the XRD pattern of $\text{Na}_{0.29}(\text{H}_2\text{O})_{0.41}\text{CoO}_{1.78}$ is similar to that of the parent compound γ - $\text{Na}_{0.7}\text{CoO}_2$, but shows a few differences as described as the following: (1) the (002) peak shifts to a lower 2θ , indicating a slight elongation of the c -axis; (2) a broad hump is observed at $2\theta \approx 23^\circ$; and (3) the (100) peak at $2\theta \approx 46.5^\circ$ shows a peak splitting. All these changes indicate a slight structural modification, which in turn would affect the relative energy band positions.

Kinetics of the topotactic transformation. The transformation from the non-hydrate phase ($c \approx 11.2$ Å) to the fully hydrated phase ($c \approx 19.6$ Å) in both of the 0.05X and 0.1X samples suggests that the whole process is slow at low concentration of KMnO_4 solution. It is known that the oxidation reaction follows the second order kinetics at low concentration of KMnO_4 solution, which means the reaction rate depends on both the concentration of the oxidized compound and the aqueous KMnO_4 solution. At low concentration of KMnO_4 solution, this could make the oxidation process slow, and in turn slow down completing the formation of fully hydrated phase. This is evidenced by the fact in our systematic study by immersing γ - $\text{Na}_{0.7}\text{CoO}_2$ in different concentrations of aqueous KMnO_4 solution for different periods of time. As shown in Fig. 7, the $c \approx 19.6$ Å phase has already appeared after one-day immersion for the 0.3X (the second category) and 1X sample (the third category). The 0.05X sample (the first category) appears only as the non-hydrate phase ($c \approx 11.2$ Å). Moreover, as shown in Fig. 8, the $c \approx 19.6$ Å phase shows up after 2 days of immersion for the 0.05X sample. It can be readily seen that the amount of non-hydrate phase existing in the sample is smaller for a larger X sample based on the relative reflection intensity of $I_{\text{max}}(c \approx 19.6 \text{ Å})/I_{\text{max}}(c \approx 11.2 \text{ Å})$. Besides, for the 0.05X sample already immersed in the KMnO_4 solution for 5 days, a small amount of non-hydrate phase is still remains after additional 4 days of exposure to the water vapor. All these results

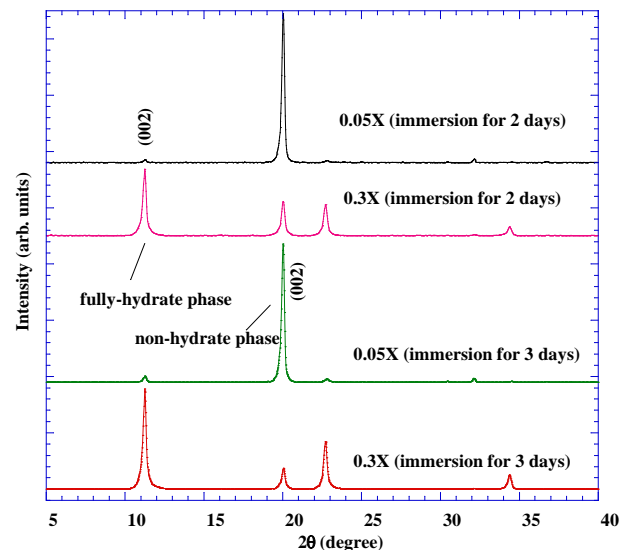
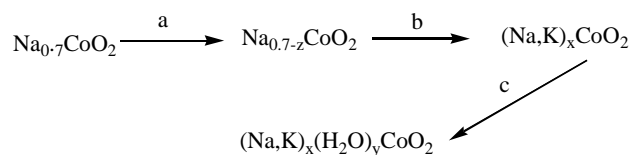


Figure 8. Powder x-ray diffraction patterns of the 0.05X and 0.3X samples, which are obtained by immersing γ - $\text{Na}_{0.7}\text{CoO}_2$ in aqueous KMnO_4 solution for 2 days and 3 days, respectively. The fully hydrate phase ($c \approx 19.6$ Å) appears after 2-day immersion in the aqueous KMnO_4 solution for the 0.05X sample. Formation of the $c \approx 19.6$ Å phase for the 0.05X sample is much slower than that of the 0.3X sample.

Scheme 1^a



^a(a) de-intercalation and oxidation process: MnO_4^- (aq) at room temperature; (b) ion exchange reaction: K^+ (aq) at room temperature and $x < 0.7$; (c) hydration process: H_2O at room temperature.

suggest that the hydration reaction in intercalating water molecule into the host lattice is a slow process. For a higher X sample ($\geq 0.3X$), the non-hydrate phase would not be observed after 5 days of aqueous KMnO_4 treatment.

Due to the presence of potassium, we propose the following scheme to describe the formation of the new phase $(\text{Na},\text{K})_x(\text{H}_2\text{O})_y\text{CoO}_2$ involving an ion exchange reaction in addition to the de-intercalation and hydration process.

The XANES spectrum. As shown in Table I, the manganese is also present in all the samples based on the ICP-AES chemical analyses. It can be seen that the relative molar ratio of Mn/Co has the similar value of 0.07-0.08 for all X samples except the 0.05X one. Efforts to wash off the remaining Mn are unsuccessful. The presence of Mn could be partly due to the aqueous permanganate solution oxidizing the water and producing the amorphous MnO_2 ¹⁹, which is confirmed by the fact that the diffraction peaks of crystalline MnO_2 show up upon heating the 10X sample. On the other hand, according to our recent results of x-ray absorption near edge structure (XANES) shown in Fig. 9, Mn does not exist in the form of MnO_4^- and its valence state in our samples is close to 4+ as compared to the absolute values of threshold energy (E_0) of different manganese oxides.²⁰⁻²² The E_0 is obtained from the

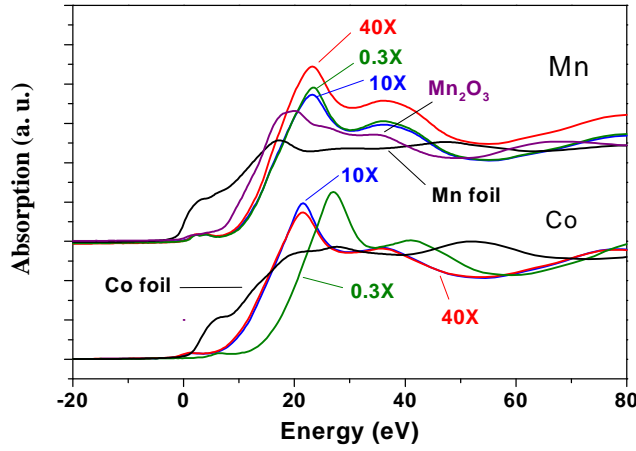


Figure 9. The normalized XANES of Mn and Co K-edge for the 0.3X, 10X and 40X samples. The intensity of each sample is normalized to edge jump equal to one.

first derivative of the near edge spectra. The absolute values of E_0 for the cobalt oxyhydrates and reference compounds are summarized in Table II. It can be readily seen that the absolute value of E_0 of Mn K-edge for the 10X and 40X samples is very close to that of CaMnO_3 , suggesting the presence of Mn^{4+} . More importantly, a chemical shift of 3.5 eV of Co K-edge is observed for the 0.3X sample (the $c \approx 19.6$ Å phase) with respect to the 10X sample ($c \approx 13.9$ Å phase), clearly indicating a higher oxidation state of the 0.3X sample. The significant difference in the E_0 of Co K-edge is consistent with the results on the oxidation number of cobalt determined by the iodometric titration. The oxidation number of cobalt and the oxygen deficiency δ is +3.34 and 0.19, respectively, for the 10X sample of $\text{Na}_{0.07}\text{K}_{0.21}(\text{H}_2\text{O})_{0.73}\text{CoO}_{2-\delta}$. Note that the oxidation number of cobalt and the oxygen deficiency δ is +3.56 and 0.05, respectively, for the 0.3X sample of $\text{Na}_{0.33}\text{K}_{0.02}(\text{H}_2\text{O})_{1.33}\text{CoO}_{2-\delta}$. These data might reveal important information about the phase formation of the cobalt oxyhydrates. For the $c \approx 19.6$ Å phase, one of the hydrogen of the H_2O molecule between the CoO_2 layers and the Na ions is hydrogen bonded an oxygen atom in the CoO_2 layers²³, which should be responsible for stabilizing the hydrated structure of bilayers of water in the lattice. Therefore, in addition to the size effect of the alkaline metal, the oxygen deficiency of $\delta = 0.19$ in $\text{Na}_{0.07}\text{K}_{0.21}(\text{H}_2\text{O})_{0.73}\text{CoO}_{2-\delta}$ might play a role being unable to stabilize the H_2O molecule between the CoO_2 layers and the Na ions, and instead leads to formation of the $c \approx 13.9$ Å phase. Since the EXAFS spectra can provide radial structural

Table II. Threshold energies (E_0) for pure Mn, Co foils, $(\text{Na},\text{K})_x(\text{H}_2\text{O})_y\text{CoO}_{2-\delta}$ synthesized using the aqueous KMnO_4 solution and the reference compounds.

Compound	E_0 , eV (Mn)	E_0 , eV (Co)
0.3X	6553.6	7728.9
10X	6554.1	7725.4
40X	6554.1	7724.8
Co foil		7709.0
CoO		7712.2
LaCoO_3 ¹⁴		7724.0
Mn_2O_3	6550.2	
MnO_2 ^{a,15}	6556.0	
$\text{La}_{0.5}\text{Ca}_{0.5}\text{MnO}_3$ ^{a,15}	6553.3	
CaMnO_3 ^{a,15}	6554.8	

^aThe threshold energy is obtained from the inflection point of the edge.

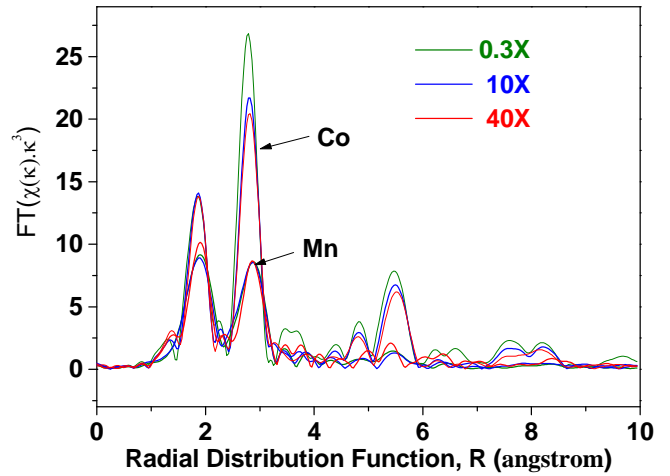


Figure 10. The Fourier Transform of $\chi(k)k^3$, derived from the k^3 -weighted EXAFS spectra, as a function of the radial distribution function for the 0.3X, 10X and 40X samples.

information about the central atom's neighbors, including the central atom-neighbors distances and the coordination number of neighbors. In order to clarify whether the Mn replaces the Co in the CoO_2 layers, we have performed the analyses on the EXAFS data to obtain the information on the bond distance and the coordination number of Mn and Co. As shown in Fig. 10, the first and second shells appear at ~ 1.9 and ~ 2.8 Å in the radial distribution function (RDF). The ratio of the integrated intensity for the first shell to that for the second shell is close to 1:2 for the Co K-edge, whereas the ratio is 1:1 for the Mn K-edge in the RDF. This result suggests that the local environment of the Mn is different from that of the Co. Therefore, the substitution of Mn for Co in our KMnO_4 -prepared samples is unlikely.

Conclusion

We have synthesized the potassium sodium cobalt oxyhydrates $(\text{Na},\text{K})_x(\text{H}_2\text{O})_y\text{CoO}_{2-\delta}$ using the aqueous KMnO_4 solution. Formation of the $(\text{Na},\text{K})_x(\text{H}_2\text{O})_y\text{CoO}_{2-\delta}$ involves not only de-intercalation, oxidation, and hydration but also an ion exchange reaction. De-intercalation of Na^+ can be simply achieved by immersing $\gamma\text{-Na}_{0.7}\text{CoO}_2$ in the tap water, which indicates that de-intercalation of Na^+ is not necessarily brought about by oxidation, instead it should be associated with the escape tendency of the Na^+ of the 2b site due to its stronger Na-Co Coulomb repulsion. When using high molar ratio of KMnO_4/Na (≥ 4.286) to treat $\gamma\text{-Na}_{0.7}\text{CoO}_2$, it would lead to significant removal of Na^+ and a pure $c \approx 13.9$ Å phase with a monolayer of water locating within the alkaline layer as a result of partial or almost complete substitution of K^+ for Na^+ . The hydration is a very slow process particularly when using aqueous KMnO_4 solution with a low molar ratio of KMnO_4/Na . According to the Co K-edge of the XANES spectra, the oxidation number of Co for the 0.3X sample of $\text{Na}_{0.33}\text{K}_{0.02}(\text{H}_2\text{O})_{1.33}\text{CoO}_{1.95}$ ($c \approx 19.6$ Å) is higher than that of the 40X sample of $\text{Na}_{0.07}\text{K}_{0.21}(\text{H}_2\text{O})_{0.73}\text{CoO}_{1.81}$ ($c \approx 13.9$ Å) with a chemical shift of 4.1 eV, which is consistent with the iodometric titration analyses with $\text{Co}^{3.56+}$ for the 0.3X sample as compared to $\text{Co}^{3.34+}$ for the 10X sample. The oxygen deficiency $\delta = 0.19$ for the 10X sample might be responsible for being unable to form the $c \approx 19.6$ phase due to being unable to stabilize the hydrated structure of bilayers of water molecule in the lattice.

Acknowledgment. This work is supported by the National Science Council of ROC, grant Nos. NSC 92-2112-M-018-005 and NSC 93-2112-M-018-003.

REFERENCES

- (1) Takada, K.; Sakurai, H.; Takayama-Muromachi, E.; Izumi, F.; Dilanian, R. A.; Sasaki, T. *Nature* **2003**, 422, 53.
- (2) Terasaki, I.; Sasago, Y.; Uchinokura, K. *Phys. Rev. B* **1997**, 56, R12685.
- (3) Fouassier, C.; Matejka, G.; Reau, J.-M.; Hagenmuller, P. *J. Solid State Chem.* **1973**, 6, 532.
- (4) Motohashi, T.; Ueda, R.; Naujalis, E.; Tojo, T.; Terasaki, I.; Atake, T.; Karppinen, M.; Yamauchi, H. *Phys. Rev. B* **2003**, 67, 064406.
- (5) Ong, N. P.; Cava, R. J. *Science* **2004**, 305, 52.
- (6) Liu, C.-J.; Liao, C.-Y.; Huang, L.-C.; Su, C.-H.; Neeleshwar, S.; Chen, Y.-Y.; Liu, C.-J. C. *Physica C* **2004**, 416, 43.
- (7) Liu, Chia-Jyi; Hung, Wen-Chin; Wang, Jung-Sheng; Liu, Chia-Jung Charlie *J. Am. Chem. Soc.* **2005**, 127, 830.
- (8) Liu, Chia-Jyi; Liao, C.-Y.; Neeleshwar, S.; Chen, Y.-Y.; Liu, Chia-Jung Charlie cond-mat/0407420.
- (9) Foo, M. L.; Schaak, R. E.; Miller, V. L.; Klimczuk, T.; Rogado, N. S.; Wang, Y.; Lau, G. C.; Craley, C.; Zandbergen, H. W.; Png, N. P.; Cava, R. J. *Solid State Commun.* **2003**, 127, 33.
- (10) Liu, C.-J.; Liao, C.-Y.; Huang, L.-C.; Su, C.-H.; Hung, W.-C.; Neeleshwar, S.; Chen, Y.-Y.; Liu, Chia-Jung Charlie *Chin. J. Phys.* **2005**, 43, 547.
- (11) Zabinsky, S. I.; Rehr, J. J.; Ankudinov, A.; Albers, R. C.; Eller, M. *Phys. Rev. B* **1995**, 52, 2995.
- (12) Lerf, A and Schöhlhorn, R. *Inorg. Chem.* **1977**, 16, 2950.
- (13) Karppinen, Maarit; Asako, Isao; Motohashi, Teruki; Yamauchi, Hisao *Chem. Mater.* **2004**, 16, 1693.
- (14) Venkatraman, S.; Manthiram, A. *Chem. Mater.* **2002**, 14, 3907.
- (15) Chebiam, R. V.; Prado, F.; Manthiram, A. *Chem. Mater.* **2001**, 13, 2951.
- (16) Karppinen, Maarit; Asako, Isao; Motohashi, Teruki; Yamauchi, Hisao *Phys. Rev. B* **2005**, 71, 092105.
- (17) Zou, Liang-Jian; Wang, J.-L.; Zeng, Z. *Phys. Rev. B* **2004**, 69, 132505.
- (18) Liu, C.-J.; Mays, M. D.; Cowan, D. O.; Sánchez, M. G. *Chem. Mater.* **1991**, 3, 495.
- (19) Skoog, D. A.; West, D. M., *Fundamental of Analytical Chemistry*, 3rd ed. Holt, Rinehart and Winston, Inc.: New York, 1976; p. 341.
- (20) Bianconi, A. *Phys. Rev. B*, **1991**, 43, 6885.
- (21) Haas, O.; Struis, R. P. W. J.; McBreen, J. M. *J. of Solid State Chemistry*, **2004**, 177, 1000.
- (22) Subias, G; García, J.; Proietti, M. G.; and Blasco, J. *Phys. Rev. B* **1997**, 56, 8183.
- (23) Jorgensen, J. D.; Avdeev, M.; Hinks, D. G.; Burley, J. C.; Short, S. *Phys. Rev. B* **2003**, 68, 214517.
- (24) Liu, Chia-Jyi; Hung, Wen-Chin, unpublished.

